JGR Atmospheres

RESEARCH ARTICLE
10.1029/2021JD036215

Differences in Ozone and Particulate Matter Between Ground Level and 20 m Aloft are Frequent During Wintertime Surface-Based Temperature Inversions in Fairbanks, Alaska

Meeta Cesler-Maloney[1], William R. Simpson[1], Tate Miles[1], Jingqiu Mao[1], Kathy S. Law[2], and Tjarda J. Roberts[3]

[1]Department of Chemistry and Biochemistry and Geophysical Institute, University of Alaska Fairbanks, Fairbanks, AK, USA, [2]LATMOS/IPSL, UVSQ, CNRS, Sorbonne Université, Paris, France, [3]Laboratoire de Physique et de Chimie de l'Environnement et de l'Espace, CNRS, Université d'Orléans, Orléans, France

Abstract During winter in Fairbanks, Alaska, fine particulate matter ($PM_{2.5}$) accumulates to large concentrations at breathing level; yet little is known about atmospheric composition aloft. To investigate vertical differences of pollutants, we measured $PM_{2.5}$ and ozone (O_3) at 3 and 20 m above ground level (AGL) in Fairbanks during winter (November 2019–March 2020). We measured temperature and $PM_{2.5}$ at 3, 6, 9, and 11 m AGL on a tower to quantify surface-based temperature inversions (SBIs) and near-surface $PM_{2.5}$ gradients. We defined SBIs as data with an 11 m minus 3 m temperature difference greater than 0.5°C. We observed the largest differences in $PM_{2.5}$ and O_3 when SBIs were present. During SBIs, $PM_{2.5}$ accumulated to large concentrations at 3 m but to a lesser extent at 20 m, demonstrating reduced vertical mixing. During SBIs, the median $PM_{2.5}$ concentration was 4.8 μg m^{-3} lower at 20 m than at 3 m. When $PM_{2.5}$ concentrations were large at 3 m, O_3 was often completely chemically removed (titrated) but was still present at 20 m. During SBIs, the O_3 mixing ratio was more than 2 nmol mol^{-1} larger at 20 m than at 3 m in 48% of the data. Results show that during SBIs, pollution in Fairbanks is mixed to altitudes below 20 m AGL and that the oxidation regime of the atmosphere changes from 3 to 20 m AGL as large differences in O_3 mixing ratios were measured during SBIs.

Plain Language Summary Temperature inversions often trap pollution emitted near ground level in high latitude cities leading to poor air quality and adverse health effects. Fairbanks, Alaska, has particularly intense temperature inversions and poor wintertime air quality caused by local sources. Here we show that during surface-based temperature inversions, particulate matter accumulates to a greater extent at 3 m above ground level than 20 m aloft. We also show that ozone, a key atmospheric oxidizer, differs on this short vertical scale during surface-based inversions, altering atmospheric chemistry aloft. This work points out the coupling between meteorological conditions, pollution and its emission altitude, and atmospheric pollution chemistry and that this coupling occurs on very short vertical length scales (~20 m) during strong temperature inversion events.

Key Points:

- During surface-based inversion events, the $PM_{2.5}$ concentration was 4.8 μg m^{-3} larger (median) at 3 m above ground level than at 20 m
- Titration of ozone was more frequent at 3 m than at 20 m, indicating oxidation chemistry differences with altitude
- Vertical differences in $PM_{2.5}$ concentration and ozone were greatest during surface-based inversion events

Supporting Information:

Supporting Information may be found in the online version of this article.

Correspondence to:

W. R. Simpson,
wrsimpson@alaska.edu

Citation:

Cesler-Maloney, M., Simpson, W. R., Miles, T., Mao, J., Law, K. S., & Roberts, T. J. (2022). Differences in ozone and particulate matter between ground level and 20 m aloft are frequent during wintertime surface-based temperature inversions in Fairbanks, Alaska. *Journal of Geophysical Research: Atmospheres*, *127*, e2021JD036215. https://doi.org/10.1029/2021JD036215

Received 16 NOV 2021
Accepted 30 APR 2022

Author Contributions:

Conceptualization: Meeta Cesler-Maloney, William R. Simpson
Data curation: Meeta Cesler-Maloney, William R. Simpson
Formal analysis: Meeta Cesler-Maloney, William R. Simpson
Funding acquisition: Meeta Cesler-Maloney, William R. Simpson, Jingqiu Mao, Tjarda J. Roberts
Investigation: Meeta Cesler-Maloney, William R. Simpson, Tate Miles, Jingqiu Mao, Kathy S. Law, Tjarda J. Roberts
Methodology: Meeta Cesler-Maloney, William R. Simpson, Tate Miles, Jingqiu Mao, Kathy S. Law, Tjarda J. Roberts
Project Administration: Meeta Cesler-Maloney, William R. Simpson, Jingqiu Mao, Kathy S. Law, Tjarda J. Roberts

1. Introduction

In Fairbanks, Alaska, (64.8°N) surface-based inversions (SBIs), where temperature increases with altitude above ground-level, are frequent during winter, occurring historically over 50% of the time from November to February/March (Bourne et al., 2010; Fochesatto & Mayfield, 2013; Tran & Mölders, 2011). These SBIs are most likely to occur in the dark winter when skies are clear as heating by incoming radiation is absent, but thermal radiation is lost continuously from the ground, leading to radiative cooling at the surface (Wendler & Jayaweera, 1972). When low-level clouds are present, they increase downwelling thermal radiation toward the surface, causing a warming effect. Therefore, clouds weaken SBIs, an effect commonly observed in Fairbanks (Bourne, 2008; Kankanala, 2007; Wendler & Jayaweera, 1972). Sunlight has potential to end an SBI, but daylight hours are short and surface heating from solar radiation is weak due to low light intensity and the high shortwave reflectivity of snow on the ground, so it is common to see SBIs persist during winter daytime in Fairbanks (Bourne, 2008; Kankanala, 2007; Tran & Mölders, 2011).

Wintertime SBIs in Fairbanks have a complex, multilayered structure. Layers of air with larger positive temperature gradients are observed from the surface to around 100 m and weaker positive gradients are observed above 100 m. In an analysis of Fairbanks radiosonde data, Fochesatto and Mayfield (2013) defined the top of the

Resources: Meeta Cesler-Maloney, William R. Simpson, Jingqiu Mao, Kathy S. Law
Software: Meeta Cesler-Maloney, William R. Simpson, Tjarda J. Roberts
Supervision: Meeta Cesler-Maloney, William R. Simpson
Validation: Meeta Cesler-Maloney, William R. Simpson, Kathy S. Law, Tjarda J. Roberts
Visualization: Meeta Cesler-Maloney, William R. Simpson
Writing – original draft: Meeta Cesler-Maloney, William R. Simpson
Writing – review & editing: Meeta Cesler-Maloney, William R. Simpson, Tate Miles, Jingqiu Mao, Kathy S. Law, Tjarda J. Roberts

inversion as the height at which temperature gradients switch from positive to negative and found an average of 377 m above the valley floor for Fairbanks winter conditions. The shallow layering of larger positive gradients seen near the surface results from radiative cooling and local flows that are influenced by topography (Fochesatto & Mayfield, 2013). Once above the topography, less stratified, weaker positive gradients are seen as distance from the surface weakens the radiative cooling effect and the influence of synoptic-scale (weather) processes becomes more influential.

Within an SBI, stability in the atmosphere is increased and vertical mixing is reduced, which has a large impact on wintertime air quality in Fairbanks. Tran and Mölders (2011), who also analyzed Fairbanks radiosonde data and defined the SBI as a positive temperature gradient with a base height starting either at the surface or below 100 m above ground level (AGL), found that all days in winter (November to February) from 2004 to 2009 with a 24-hr average $PM_{2.5} > 35$ μg m^{-3} were associated with SBIs. In contrast, there were no days when 24-hr average $PM_{2.5} > 35$ μg m^{-3} were associated with elevated inversions, which were defined as positive temperature gradients with a base height starting above 100 m AGL. These results from Tran and Mölders (2011) suggest that inversions, which begin in the first 100 m AGL, have the most influence on particulate matter ($PM_{2.5}$) concentrations at ground level.

It is important to understand how SBIs affect local air quality as exposure to $PM_{2.5}$ causes respiratory inflammation and is associated with an increase in hospital admissions for cardiovascular and respiratory illnesses (Atkinson et al., 2014; Dominici et al., 2006; Huang et al., 2012; Kossover, 2010; Silkoff et al., 2005). A review of local air pollution in the Arctic by Schmale et al. (2018) highlights the need for more information on local pollution sources in the Arctic. In addition to SBIs affecting cities and villages in Arctic regions, midlatitude locations that experience frequent SBIs also experience a decline in air quality in the winter when local emissions are present.

Fairbanks is not unique in having poor air quality during winter. In Helsinki, Finland (60°N), the amount of submicron particulate matter ($PM_{1.0}$) attributed to biomass burning increases in winter (Carbone et al., 2014). Analysis of $PM_{2.5}$ filter samples from Canada showed that 24-hr average $PM_{2.5}$ concentrations had seasonal peaks in the winter months in the Northwestern cities of Golden (51°N) and Edmonton (53°N) (Dabek-Zlotorzynska et al., 2011). Increases in ground-level particulate matter have also been correlated with temperature inversion events in Europe, China, and across the United States (Baasandorj et al., 2017; Connell et al., 2005; Pastuszka et al., 2010; Silcox et al., 2011; Tsybulski Gennady et al., 2020; Zhong et al., 2017).

There has been more opportunity to study wintertime pollution in Fairbanks than in other cities at similar latitudes. The majority of breathing-level $PM_{2.5}$ measured at 3 m AGL in Fairbanks appears to be emitted by sources near the surface, and contributions from point sources (e.g., power plants that have elevated stacks) are suggested to be small (Alaska Department of Environmental Conservation, 2016; Tran & Mölders, 2012). In a Lagrangian puff model simulation for a 17-day pollution episode in Fairbanks, where days in the episode had 24-hr average surface $PM_{2.5}$ concentrations near 41 μg m^{-3}, an episode average surface concentration of only 3.8 μg m^{-3} $PM_{2.5}$ was estimated to come from power plant sources (Alaska Department of Environmental Conservation, 2016). The contribution of point sources to ground level $PM_{2.5}$ has only been modeled thus far and has not been investigated using in-field measurements.

Sources of $PM_{2.5}$ in Fairbanks differ from sources in non-Arctic regions mostly due to differences in fuel use and the increased need for home heating at cold temperatures. A chemical mass balance source apportionment analysis by Ward et al. (2012) calculated the percentage of $PM_{2.5}$ attributed to different particulate matter sources and found that 60%–80% of $PM_{2.5}$ in downtown Fairbanks was attributed to wood combustion sources, 8%–20% to sulfate aerosol particles, 3%–11% to ammonium nitrate aerosol particles, 0%–10% to diesel exhaust sources, and 0%–7% to automobile sources. Wood combustion sources are characterized by large amounts of organic carbon as well as smaller amounts of elemental carbon and potassium. Sulfate aerosol particles, the second largest source of $PM_{2.5}$ in source apportionment analyses, can be emitted as primary particles from the combustion of sulfur containing fuels (coal, fuel oil, and high sulfur diesel fuel) or may be produced as a secondary particulate matter when gaseous or dissolved sulfur dioxide gas is oxidized. Ammonium nitrate can be formed as a secondary particulate matter when ammonia reacts with nitric acid (HNO_3). The hydrolysis of dinitrogen pentoxide (N_5O_5) can also add nitrate to $PM_{2.5}$. This dissolved nitrate, like sulfate, will acidify an aerosol unless it is neutralized by sufficient ammonia gas.

A positive matrix factorization source apportionment analysis by Y. Wang and Hopke (2014) suggested that 40.5% of $PM_{2.5}$ could be attributed to wood combustion. A later analysis by Busby et al. (2016) used ^{14}C as a wood combustion tracer as $PM_{2.5}$ emitted from modern biomass burning sources will contain ^{14}C, while $PM_{2.5}$ emitted from older fossil fuel sources will not. This analysis suggested that the average $PM_{2.5}$ mass concentration percentage attributed to wood combustion over a 3-year period ranged from 33.6% to 40.4%. Regulatory efforts were successful in reducing $PM_{2.5}$ from wood combustion in eight out of nine sites in the northwestern USA (Kotchenruther, 2020). Although Fairbanks was not in the Kotchenruther (2020) study, contributions from wood combustion to Fairbanks $PM_{2.5}$ appear to be decreasing over time and the source apportionment of $PM_{2.5}$ in Fairbanks may be changing annually due to changes in fuel use and regulatory efforts (information on air quality advisories in Alaska is found at https://dec.alaska.gov/Applications/Air/airtoolsweb/Advisories/).

These source apportionment studies all show that a majority of Fairbanks $PM_{2.5}$ are attributed to home heating sources (Busby et al., 2016; Y. Wang & Hopke, 2014; Ward et al., 2012). In a survey of Fairbanks residents from 2011 to 2015, heating oil was the most used fuel source at 70%–74% and wood was the second most used at 22%–24%. Although heating oil is more widely used in Fairbanks, wood combustion emits more $PM_{2.5}$ on a tons day^{-1} basis compared to other residential heating sources (Alaska Department of Environmental Conservation, 2016). The chemical composition of $PM_{2.5}$ will not be discussed in detail as the focus here is on vertical differences of $PM_{2.5}$ and O_3 near the surface.

In addition to $PM_{2.5}$, the mixing ratio of gases can also be affected by SBIs. The use of long-path differential optical absorption spectroscopy in the midlatitudes to remotely sense vertical distributions of O_3, NO_3, and N_2O_5 shows that these species increase with altitude during nocturnal inversions when mixing is reduced (Geyer & Stutz, 2004; Stutz et al., 2004; S. Wang et al., 2006; Wong et al., 2011). Vertical gradients in these studies dissipated during the day when mixing increased and were more well-defined when nocturnal inversions were stronger. Nocturnal gradients of N_2O_5 and HNO_3 have also been measured using chemical ionization mass spectrometry and broadband cavity enhanced absorption spectrometry in the RONOCO aircraft campaign in the United Kingdom (Le Breton et al., 2014). During these nocturnal inversions, photochemical production of O_3 is ceased and NO emitted near the ground accumulates and rapidly titrates O_3. At the same time aloft, O_3 is not fully titrated as the vertical transport of NO is hindered within the nocturnal inversion and mixing ratios of NO are smaller aloft.

Given the frequent SBIs in Fairbanks, this work was designed to investigate the relationship between SBIs and vertical gradients of both $PM_{2.5}$ and O_3 that form in the winter and early spring months. To this end, we measured differences of $PM_{2.5}$ and O_3 measured at 20 and 3 m AGL throughout the winter in downtown Fairbanks. We also measured temperature and $PM_{2.5}$ at 3, 6, 9, and 11 m AGL to investigate how differences in $PM_{2.5}$ and O_3 with altitude were related to near-surface temperature gradients. In Section 2, we discuss the methods and instrumentation used during the field study. In Section 3, we present near-surface vertical difference measurements of $PM_{2.5}$, O_3, and SBIs. In Sections 4 and 5, we discuss the influence of SBIs on vertical difference measurements and examine how these vertical differences affect the atmospheric chemistry at different altitudes.

2. Methods

2.1. Measurements of $PM_{2.5}$ and O_3 and Temperature

Measurements of $PM_{2.5}$ and O_3 were cross-calibrated against monitors located at the State of Alaska Department of Environmental Conservation National Core network (NCore) site in downtown Fairbanks (64.8458°N, 147.72727°W). Two PurpleAir (model PA-II, https://www.purpleair.com) particulate matter sensors were stationed at the University of Alaska Fairbanks Community and Technical College (CTC) building (64.84064°N, 147.72677°W) during winter from November 2019 to March 2020. Figure 1 shows a map of CTC and other locations used in this study. To measure differences in $PM_{2.5}$ with altitude, one PurpleAir was placed on the roof of the CTC building at 20 m and another was placed at the base of the building at 3 m.

Each PurpleAir contains two identical Plantower PMS5003 sensors, which report particle counts under the threshold diameter sizes of 0.3, 0.5, 1.0, 2.5, 5.0, and 10 μ based on the intensity of scattered light detected. A proprietary algorithm within the sensor converts reported counts into an equivalent concentration of $PM_{1.0}$, $PM_{2.5}$, and PM_{10} in μg m^{-3}. A recent study evaluated PurpleAir sensors using data from the National Oceanic and Atmospheric Administration's (NOAA) Mauna Loa Observatory and Boulder Table Mountain (BOS) and

Figure 1. Map of locations in the field study. At the Community and Technical College building, $PM_{2.5}$ was measured at 3 and 20 m above ground level (AGL), while O_3 was measured at 20 m AGL. At the trailer, which was moved between all locations, $PM_{2.5}$ and temperature were both measured at 3, 6, 9, and 11 m AGL.

they were found to measure and predict aerosol light scattering coefficients equivalent to that of an integrating nephelometer rather than a true particle counter (Ouimette et al., 2021). PurpleAir sensors have been shown to agree well with $PM_{2.5}$ measurements from Environmental Protection Agency (EPA)-approved monitors. In a recent analysis by Ardon-Dryer et al. (2020) 75% of their comparisons between PurpleAir and EPA Air Quality Monitoring Station data had an $R^2 > 0.8$.

The PurpleAir sensor has also proved to be a useful analytical tool as the integration of PurpleAir $PM_{2.5}$ measurements in statistical models has improved the quality of $PM_{2.5}$ predictions in urban areas (Bi et al., 2020). All PurpleAir sensors in this study were calibrated against the beta-attenuation monitors (BAMs), which measure hourly $PM_{2.5}$ at the NCore site, as described in the following section. The PurpleAir data were averaged hourly for analysis.

We measured O_3 mixing ratios on the roof of the CTC building at 20 m with a Dasibi 1008-RS O_3 analyzer. The O_3 analyzer was operated indoors in a temperature-conditioned room at the top of the CTC building sampling ambient outdoor air via a 1/4 inch outer diameter Teflon inlet running outside to the roof. The O_3 data were averaged hourly for analysis. To compare O_3 aloft to surface measurements at 3 m AGL, we used O_3 observations from the NCore site, which is 500 m north of the CTC building. Given the close horizontal proximity of the CTC building to the NCore site, we assumed that hourly averaged O_3 differences were representative of the vertical distribution of O_3 rather than horizontal differences. Analysis of 24-hr averaged $PM_{2.5}$ comparing NCore and the State Office Building (SOB, which is across the street from CTC) showed that these sites were sufficiently correlated for the EPA to allow the NCore monitor to replace the former regulatory monitor at SOB, giving further evidence that the horizontal displacement between NCore and CTC leads to little difference in air mass composition at ground level (Alaska Department of Environmental Conservation, 2016).

Temperature probes were constructed from thermistors glued inside 9-mm diameter metal tubes with epoxy. The temperature probes were placed inside an aspirated radiation shield built from concentric PVC pipes utilizing a fan to provide ventilation (Smoot & Thomas, 2013). Four temperature probes were deployed at 3, 6, 9, and 11 m AGL on a retractable tower attached to a trailer, referred to here as the "Trailer Tower." The relative precision of these temperature sensors was better than 0.15°C over the range from 20 to −60°C.

Four additional PurpleAir sensors were also deployed on the Trailer Tower at the same altitudes as the temperature probes and were cross-calibrated against the BAM $PM_{2.5}$ at the NCore site as described in the following section. The Trailer Tower was stationed at five different sites within Fairbanks during the field study. Table 1 shows the Trailer Tower locations and dates of deployment at each site. The sites in Figure 1 are less than 4 km away from the CTC building with no large changes in topography and ground elevations above sea level within 2 m of the CTC building; thus, it was assumed that similar near-surface temperature gradients were present at each location.

Table 1
Locations and Dates of Deployment for the Trailer Tower During the Field Study

Location of trailer	NCore	Trainor gate	River road	A street	CTC	NCore
Dates of deployment	1 November 2019–15 November 2019	16 November 2019–15 January 2020	15 January 2020–7 February 2020	8 February 2020–10 March 2020	10 March 2020–18 March 2020	18 March 2020–9 April 2020

2.2. Calibration and Quality Control for Measurements

At the start and end of the field study, all instruments were colocated at the NCore site for quality control. Correlation of each PurpleAir sensor's raw $PM_{2.5}$ measurement with NCore measurements was high (R typically > 0.80) and slopes were near unity. However, the difference analysis used here requires good comparability and precision, so a set of linear calibration equations were used to correct all PurpleAir sensors for improved agreement with the regulatory measurements at NCore. After correction, all PurpleAir sensors had slopes within 3% of unity of NCore $PM_{2.5}$ and a mean absolute error <2 μg m^{-3}, indicating that the linear models used were effective in calibrating the sensors (see Section S1 in Supporting Information S1 for details).

We chose to use the hourly BAM data as a common reference that allowed comparability of the PurpleAir data on an average basis. This study only makes comparisons between PurpleAir data and other PurpleAir data, such that any residual systematic errors that the PurpleAirs may have (i.e., temperature or RH dependences) would be common and do not contribute to differences in $PM_{2.5}$ concentrations at various altitudes. More information about the calibration of the PurpleAir sensors is found in Section S1 of Supporting Information S1.

Daily zero and span calibrations verified consistent operations of the Dasibi O_3 analyzer. When colocated with the NCore monitor before and after the winter, the linear regression slope (NCore O_3 vs. Dasibi O_3) was within 5% of unity and the intercept was <2 pmol mol^{-1}, indicating excellent performance. Though O_3 slopes and intercepts were good, both intercepts are positive and the slope was below unity in the first calibration and was above unity in the second calibration, so a linear correction equation was applied to the O_3 data (see Section S3 in Supporting Information S1 for details).

Temperature probes were operated in different controlled environments at around 20, 5, −20, and −60°C. During these tests, the temperature difference between each individual probe and the average of all probes was calculated for data at each set temperature and the mean temperature difference was within ±0.15°C for all probes across the 20 to −60°C range (see Section S2 in Supporting Information S1 for details).

To ensure the temperature probes on the Trailer Tower remained in agreement throughout the campaign, the tower was lowered three times, such that each temperature probe was situated at the same altitude (3 m AGL). The precision of the temperature probes was consistent throughout the study as over 80% of the data at one-minute time resolution from each probe had a ±0.15°C difference from the average temperature of all probes when the Trailer Tower was lowered.

3. Results

3.1. Characteristics of SBIs and Influence on Surface $PM_{2.5}$ Concentrations

Air temperature on the Trailer Tower ranged from a minimum of −41°C to a maximum of 5°C during the field study period. The temperature difference of 11 m minus 3 m on the Trailer Tower ($dT_{11-3\ m}$ = temperature at 11 m − temperature at 3 m) was used to quantify the intensity of the temperature gradient in the first 11 m AGL and to determine the presence of SBIs in the data. Figure 2 shows a time series and histograms of hourly 11 and 3 m temperatures and the hourly temperature difference $dT_{11-3\ m}$ from the Trailer Tower. In a neutral atmosphere where the environmental lapse rate equals the dry adiabatic lapse rate and vertical mixing occurs, the 8 m height difference across the Trailer Tower would result in a difference $dT_{11-3\ m} = -0.078$°C. This difference ($dT_{11-3\ m} = -0.078$°C) is in agreement with the narrow spike in the $dT_{11-3\ m}$ histogram in Figure 2, while many other observations had a more positive dT, indicative of a surface temperature inversion.

A temperature difference $d_{11-3\ m} > 0.5$°C was chosen as an indicator for the presence of an SBI as this is clearly different given sensor precision from the neutral stability result (Figure 2). We chose to use 11 and 3 m temperature

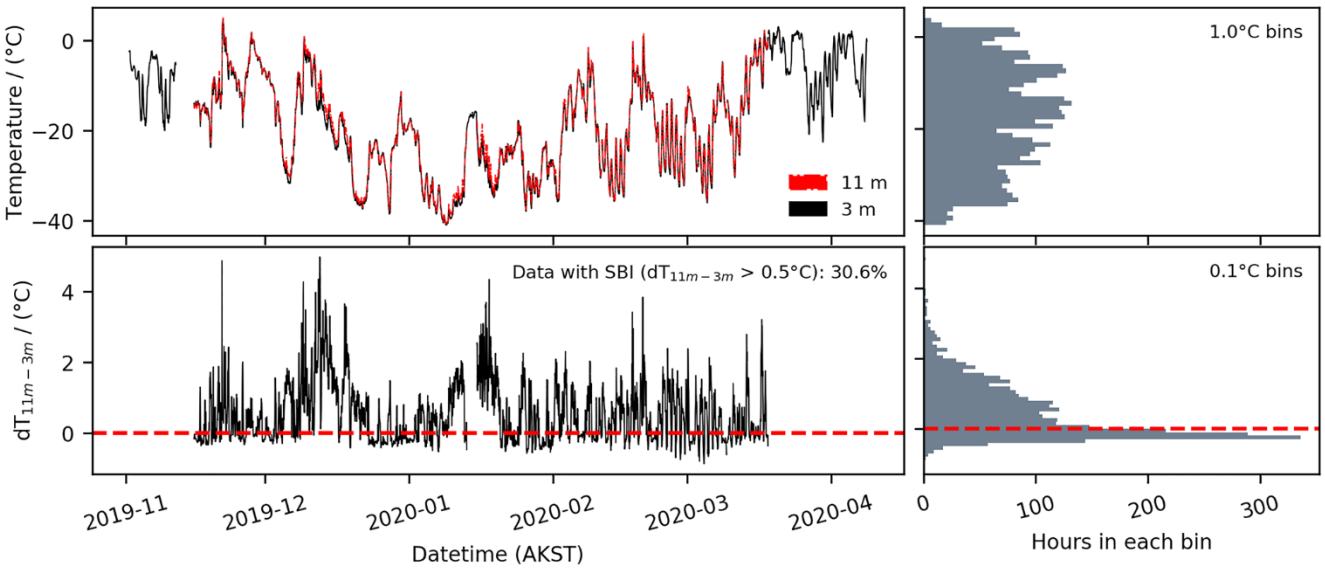

Figure 2. Time series and histograms of hourly 11 and 3 m temperature and hourly temperature difference $dT_{11-3\,m}$ at the Trailer Tower. The dashed line on $dT_{11-3\,m}$ plots is at 0°C.

data in our definition of an SBI because they have the largest vertical difference and thus provide the largest signal to noise when defining SBIs (see Figure S11 in Supporting Information S1). The positive temperature gradient during these SBIs likely extends past 11 m altitude above the 11 m vertical scale of our tower; however, it was not our goal here to determine the maximum height of the SBI layer. The Figure 2 histogram also clearly demonstrates by its asymmetry that the positive temperature differences are much larger than the negative ones. Our choice to use a temperature difference $dT_{11-3\,m} > 0.5$°C is quite conservative. Our calibrations and in-field validations (discussed in Section S2 of Supporting Information S1) show that our temperature probes are precise to each other within about 0.1°C (mean absolute error of all sensors <0.05°C), so the observed temperature differences up to ~3°C in our data are well outside errors.

At the Trailer Tower, 30.6% of the data showed evidence of an SBI where $dT_{11-3\,m} > 0.5$°C. Figure 3 shows a time series of $PM_{2.5}$ mass concentrations colored by the presence or absence of SBI. The EPA ambient air quality standard thresholds for $PM_{2.5}$ were used as a reference in Figure 3, where $PM_{2.5} > 12$ μg m^{-3} is above the annual standard, $PM_{2.5} > 35$ μg m^{-3} is above the 24-hr standard, and $PM_{2.5} > 55$ μg m^{-3} is considered "unhealthy" for all people. Table 2 shows the probability of observing an SBI when $PM_{2.5}$ was greater than 12, 35, and 55 μg m^{-3} at the CTC building. Figure 4 shows that SBIs occurred across a wide range of temperatures but were more frequent at lower temperatures though there was a reduction in the frequency of SBIs at extremely cold temperatures around −40°C.

To validate our assumption that similar near-surface temperature gradients were present across all Trailer Tower locations in the study, we compared the near-surface temperature gradients at the NCore site and the Trailer Tower using our SBI detection method. The NCore site temperatures were measured at two altitudes, 2 and 10 m AGL, so instead of the temperature difference $dT_{11-3\,m}$ that was used to detect SBIs at the Trailer Tower, the 10 m minus 2 m temperature difference ($dT_{10-2\,m}$) was used to detect SBIs at the NCore site (SBIs detected at NCore when $dT_{10-2\,m} > 0.5$°C). There were SBIs detected at both sites in 53% of the data and SBIs were detected at neither site in 32% of the data, meaning 85% of the data agreed between sites using our SBI detection method.

3.2. Differences in $PM_{2.5}$ Concentration With Altitude

Figure 5 shows the correlation of 20 and 3 m $PM_{2.5}$ at the CTC building (right panel) and the correlation of 11 and 3 m $PM_{2.5}$ at the Trailer Tower (left panel). When the temperature difference $dT_{11-3\,m}$ was near zero, $PM_{2.5}$ at 20 and 3 m were well-correlated at the CTC building in Figure 5 (right panel), appearing close to the one-to-one line. Data in Figure 5 (right panel) that had a larger temperature difference $dT_{11-3\,m}$, indicating a stronger SBI, had larger $PM_{2.5}$ concentrations at 3 m than at 20 m as measurements with a larger $dT_{11-3\,m}$ generally lie below

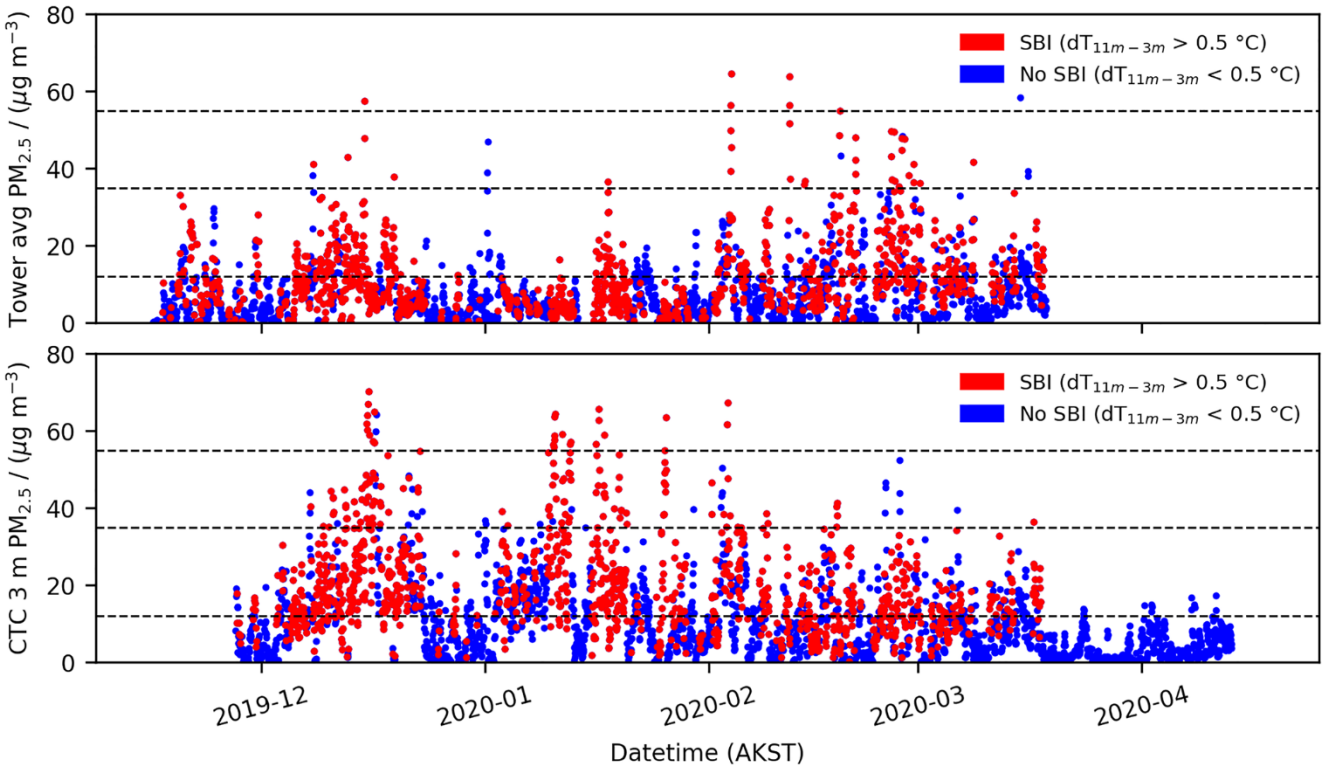

Figure 3. Time series of $PM_{2.5}$ concentration from the Trailer Tower (average of 3, 6, 9, and 11 m $PM_{2.5}$, top) and the Community and Technical College building (bottom) colored by the presence of surface-based temperature inversions where $dT_{11-3\,m} > 0.5°C$. Three Environmental Protection Agency-based thresholds are shown as dashed lines.

the one-to-one line. Figure 6 shows that $PM_{2.5}$ concentration differences at the CTC building ($dPM_{20-3\,m} = PM_{2.5}$ at 20 m − $PM_{2.5}$ at 3 m) are more frequently negative than positive. In Figure 6 (left panel), a smaller but opposite effect was observed on the shorter Trailer Tower, where negative $PM_{2.5}$ differences ($dPM_{11-3\,m} = PM_{2.5}$ at 11 m − $PM_{2.5}$ at 3 m) were marginally less frequent than positive differences.

The percentage of time differences $dPM_{20-3\,m}$ and $dPM_{11-3\,m}$ was above +5 μg m^{-3} or below −5 μg m^{-3} and is shown in Table 3. The thresholds of ±5 μg m^{-3} in Figure 6 and Table 3 were chosen to account for instrument noise in the difference measurements. Comparing the full data set to a selection of data where SBIs with $dT_{11-3\,m} > 0.5°C$ were present, the percentage of data at the CTC building where $dPM_{20-3\,m} < -5$ μg m^{-3} increased from 16.7% to 45.6% in the SBI selected data set. In contrast, the percentage of data where $dPM_{20-3\,m} > 5$ μg m^{-3} only increased from 1.85% to 2.17% in the SBI selected data set. For the shorter Trailer Tower, differences of $PM_{2.5}$ where $dPM_{11-3\,m} > 5$ μg m^{-3} were more frequent at the Trailer Tower compared to the CTC building both with and without coincident SBIs. Although the percentage of $PM_{2.5}$ differences where $dPM_{11-3\,m} < -5$ μg m^{-3} also increased in the SBI selected data set at the Trailer Tower, the increase was not as large as the increase observed at the taller CTC building in Table 3.

Table 2
Percentage of Hourly $PM_{2.5}$ Concentrations Above a Given Threshold Coincident With a Temperature Difference $dT_{11-3\,m} > 0.5°C$ Over the Entire Field Campaign (1 November 2019–18 March 2020)

CTC building (3 m)	Probability of $PM_{2.5} > 12$ μg m^{-3}	Probability of $PM_{2.5} > 35$ μg m^{-3}	Probability of $PM_{2.5} > 55$ μg m^{-3}
	32.5%	4.09%	0.69%
SBI probability (all data)	SBI probability of $PM_{2.5} > 12$ μg m^{-3}	SBI probability of $PM_{2.5} > 35$ μg m^{-3}	SBI probability of $PM_{2.5} > 55$ μg m^{-3}
30.6%	61.9%	82.5%	92.8%

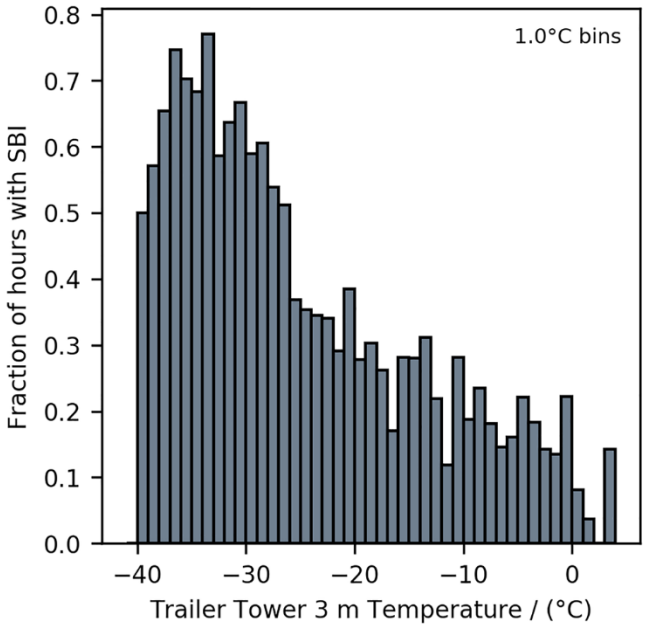

Figure 4. Histogram of the fraction of hours with an surface-based temperature inversion ($dT_{11-3\ m} > 0.5$°C) to the total number of hours as a function of 3 m temperature on the Trailer Tower.

Figure 7 shows that the median difference $dPM_{20\ m-3\ m}$ during SBIs at the CTC building was −4.8 μg m^{-3}. For 8 days from 10 March 2020 to 18 March 2020, the Trailer Tower was colocated at the CTC building. To compare intra-tower $PM_{2.5}$ concentration differences, the difference between $PM_{2.5}$ at altitude Ln on the Trailer Tower minus the Trailer Tower average $PM_{2.5}$ ($dPM_{[Ln - Lavg]}$) was calculated. Figure 8 shows the median differences from the Trailer Tower, $dPM_{[Ln - Lavg]}$, and the median differences from the CTC building roof, $dPM_{20-3\ m}$, in the SBI selected data set during the period of colocation. Intra-tower $PM_{2.5}$ concentration differences $dPM_{[Ln - Lavg]}$ were smaller at all altitudes on the Trailer Tower than the median $PM_{2.5}$ concentration difference $dPM_{20-3\ m}$ of −4.5 μg m^{-3} measured at the CTC building during the 8-day period of colocation in Figure 8.

3.3. Differences in O_3 With Altitude

The correlation plot for 20 and 3 m O_3 at the CTC building showed minimal differences when the temperature difference $dT_{11-3\ m}$ was near zero. Figure 9 shows that the most O_3 data during periods without an SBI lie near the one-to-one line. When SBIs were present, 3 m O_3 mixing ratios were typically near zero, while O_3 mixing ratios at 20 m were still present at mixing ratios of 20–30 nmol mol^{-1} and O_3 differences were greater when SBIs were stronger. There were however periods when $dPM_{20-3\ m}$ was large and O_3 was near zero at both 3 and 20 m. Considering O_3 differences at the CTC building ($dO3_{20-3\ m}$ = O_3 at 20 m minus O_3 3 m), Figure 10 shows that positive differences were more frequent than negative differences. Table 4 shows the percentage of data where $dO3_{20-3\ m}$ was above +2 nmol mol^{-1} or below −2 nmol mol^{-1}. The thresholds of ±2 nmol mol^{-1} in Figure 10 and Table 4 were chosen to account for instrument noise in the difference measurements. Comparing the full data set to a selection of data where SBIs were detected by our method

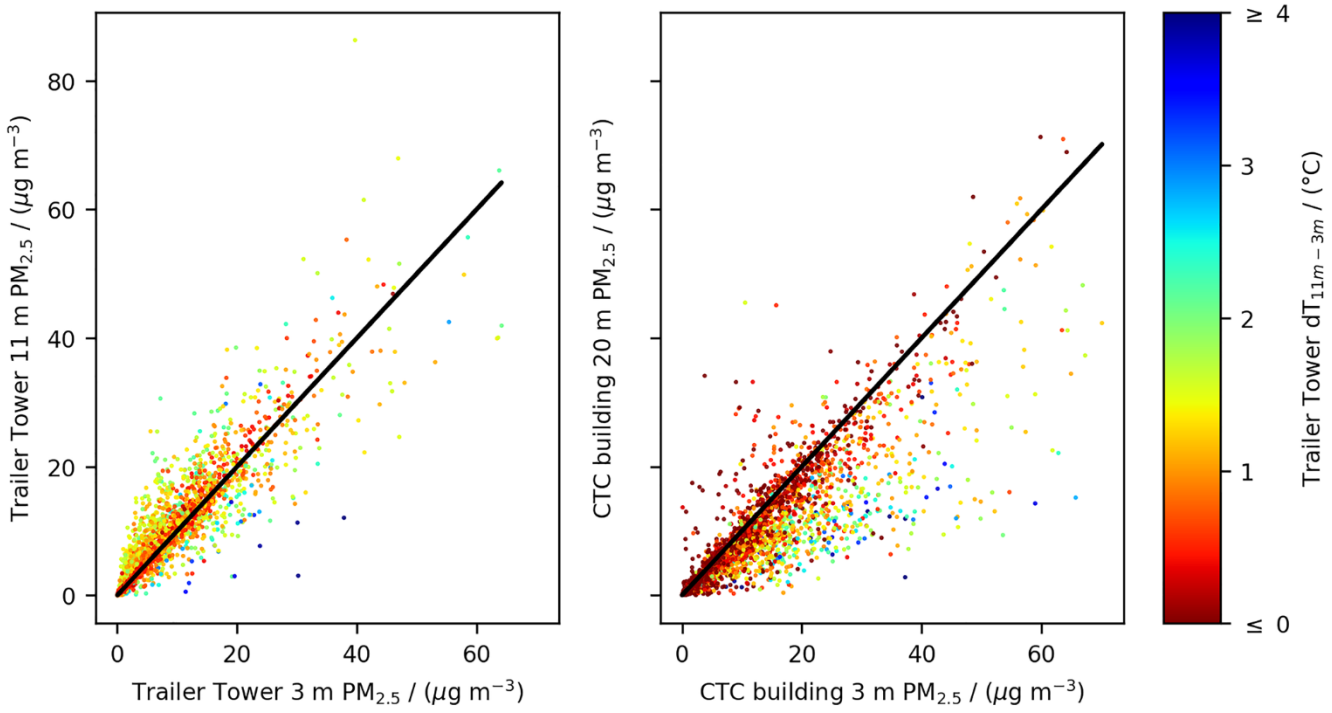

Figure 5. 20 versus 3 m $PM_{2.5}$ at the Community and Technical College building (left) and 11 versus 3 m $PM_{2.5}$ at the Trailer Tower (right) colored by $dT_{11-3\ m}$ to show surface-based temperature inversion intensity.

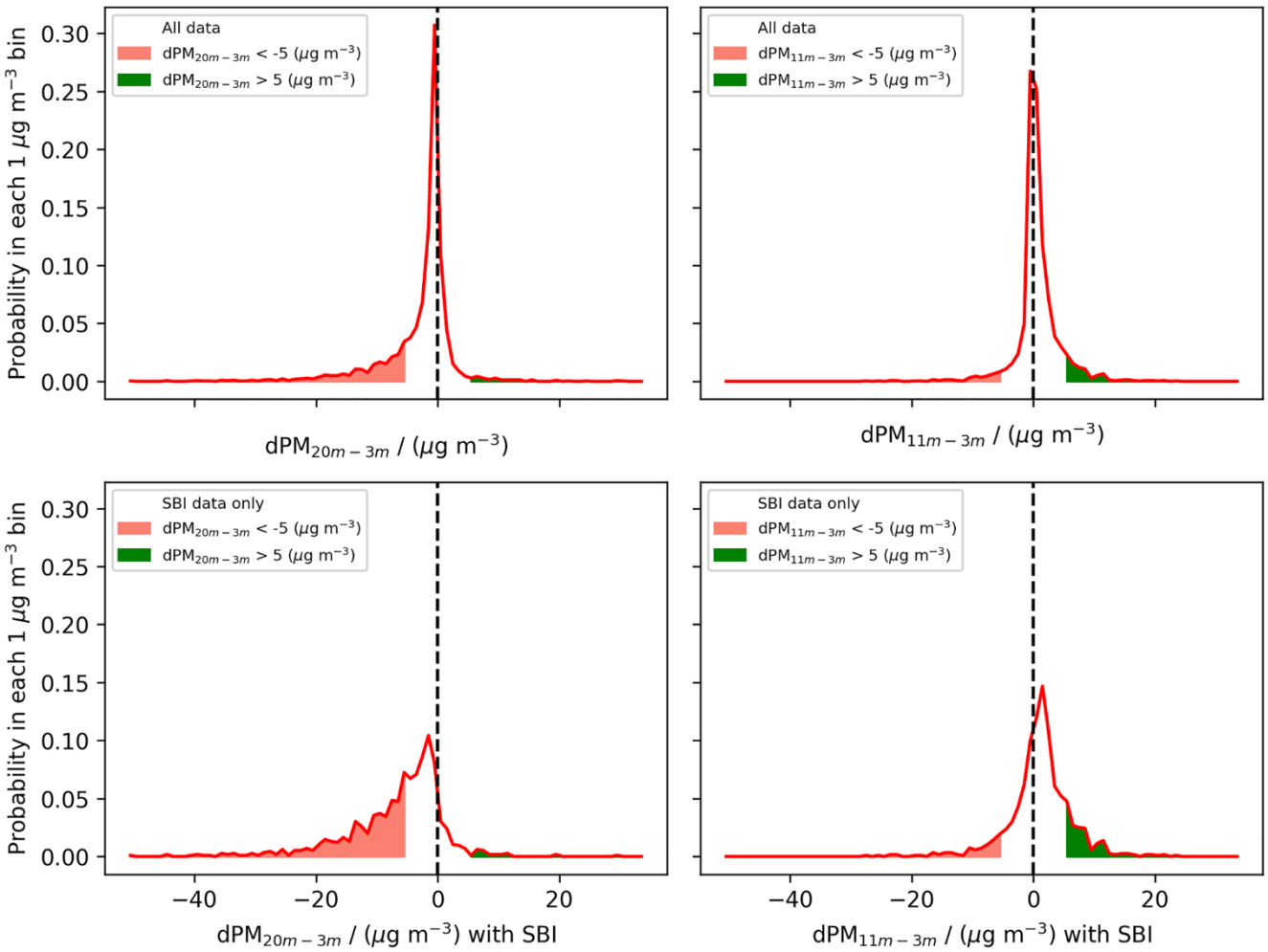

Figure 6. Histograms of $PM_{2.5}$ differences at the Community and Technical College building and the Trailer Tower. The top row is for all data, while the bottom row is for periods where surface-based temperature inversion was present.

($dT_{11-3\,m} > 0.5°C$), the percentage of data with positive O_3 differences $dO3_{20-3\,m}$ increased from 26.3% to 48.2% in SBI-selected data, while the percentage of data with negative O_3 differences $dO3_{20\,m-3\,m}$ decreased from 2.51% to 0.97%.

4. Discussion

4.1. Characteristics of SBIs in Fairbanks

Throughout the field study, SBIs were frequent, occurring near one-third of the time. Figure 4 shows that there was an increase in the frequency of SBIs at colder surface temperatures. Colder surface temperatures are often associated with clear sky conditions during the winter in Fairbanks as thermal radiation from the surface is lost while skies are clear and the ground becomes colder. When temperatures are approximately below −30°C, ice

Table 3
Percentage of Time $PM_{2.5}$ Differences $dPM_{20-3\,m}$ and $dPM_{11-3\,m}$ Above or Below 5 μg m^{-3}

	$dPM_{20-3\,m} < -5$ μg m^{-3}	$dPM_{20-3\,m} > +5$ μg m^{-3}	$dPM_{11-3\,m} < -5$ μg m^{-3}	$dPM_{11-3\,m} > +5$ μg m^{-3}
All data	16.7%	1.85%	2.81%	6.02%
Data with SBI	45.6%	2.17%	8.46%	17.16%

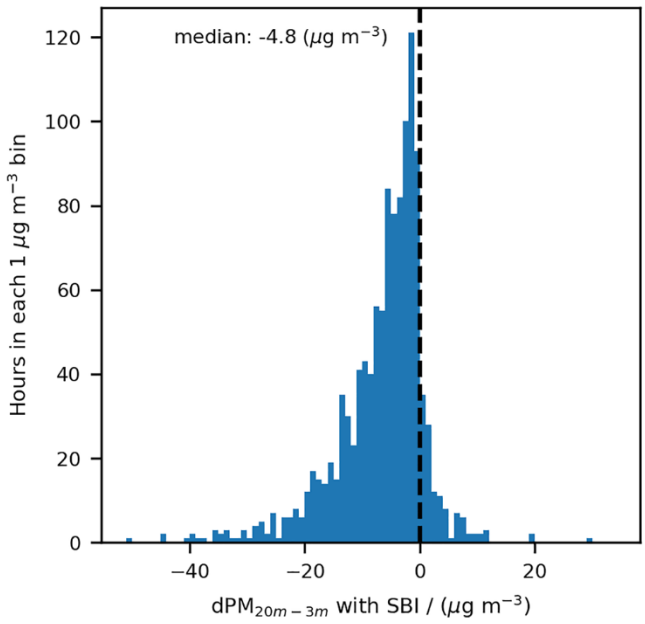

Figure 7. Histogram of $PM_{2.5}$ difference $dPM_{20-3\ m}$ at the Community and Technical College building when $dT_{11-3\ m} > 0.5°C$.

fog may precipitate from humid air that is trapped near the surface (Robinson et al., 1956; Schmitt et al., 2013). In a January 2012 ice fog event in Fairbanks, the measured SBI weakened in intensity after the precipitation of ice fog occurred (Schmitt et al., 2013). Ice fog is often optically thick such that the top of the ice fog layer becomes the radiative cooling interface and the ice fog layer becomes convective, thus decreasing the SBI intensity, which could explain the slight decrease (Figure 4) in the fraction of hours with an SBI at severely cold temperatures (Robinson et al., 1956).

Our SBI criterion of $dT_{11-3\ m} > 0.5°C$ differs from that of Fochesatto and Mayfield (2013), who used a threshold gradient of 0.1°C per 100 m altitude difference (equivalent to $dT_{11-3\ m} = 0.008°C$) and from Tran and Mölders, who did not use a threshold. Our choice of SBI criterion means that fewer SBIs will be detected by our method than by Fochesatto and Mayfield (2013) (64%) or Tran and Mölders (2011) (75%). For our study, it was necessary to have hourly SBI statistics, which are not possible from the every-twelve-hour radiosonde data used in these other studies, so differences in SBI probabilities are to be expected. Figure 3 and Table 2 show that we detect enough SBIs with this method to show statistical significance in the relationship between SBIs and $PM_{2.5}$ pollution events.

4.2. Differences of $PM_{2.5}$ at the CTC Building and Trailer Tower

Across the taller height difference probed at the CTC building, a majority of $PM_{2.5}$ differences $dPM_{20-3\ m}$ were negative and there was as much as 50 μg m^{-3} less $PM_{2.5}$ measured at 20 m than at 3 m. In contrast to the shorter Trailer Tower, $PM_{2.5}$ differences $dPM_{11-3\ m}$ across the 11-m tall Trailer Tower were both positive and negative, and the range of $dPM_{11-3\ m}$ generally did not exceed ±10 μg m^{-3}. Measurements of $PM_{2.5}$ at the CTC building show that pollution in Fairbanks is often only mixed at altitudes <20 m in the winter and that large $PM_{2.5}$ differences are common between 20 m AGL and lower altitudes.

Within the first 11 m AGL, $PM_{2.5}$ differences were smaller than the first 20 m AGL in Figures 5 and 8, suggesting that a more mixed layer could be present between the surface and 11 m as compared to the surface to 20 m AGL probed at CTC. Large obstructions (buildings and trees) and moving objects can increase mechanical mixing near the surface, which could explain why $PM_{2.5}$ appears more mixed from 3 to 11 m. Although $PM_{2.5}$ appears more mixed from 3 to 11 m when looking at the median $dPM_{[Ln-Lavg]}$ at each altitude, Figure 4 shows that some large differences in $PM_{2.5}$ were observed episodically as may be expected in a stratified but periodically mixed environment.

4.3. Influence of SBIs on $PM_{2.5}$ and O_3 Differences

For both $PM_{2.5}$ and O_3, vertical differences over 20 m at the CTC building were the most pronounced when SBIs were detected. Although $PM_{2.5}$ did not accumulate to large concentrations every time there was an SBI, Table 2 shows that there was almost always an SBI when $PM_{2.5}$ exceeded the EPA ambient air quality standards, consistent with previous studies (Tran & Mölders, 2011). The correlation of $PM_{2.5}$ at 20 and 3 m was poor when SBIs were present (as shown in Figure 5), consistent with greater accumulation of $PM_{2.5}$ at 3 m than at 20 m. Large negative $PM_{2.5}$ concentration differences with increasing altitude to 20 m were more frequent during SBIs as Table 3 shows that selecting for SBIs increased the probability of large reductions in $PM_{2.5}$ at 20 m as compared to 3 m ($dPM_{20-3\ m} < -5$ μg m^{-3}), which increased from 16.7% to 45.6% with SBIs present. These results suggest that during an SBI when the atmosphere has increased stability, $PM_{2.5}$ becomes stratified and vertical mixing of pollution is hindered at altitudes below 20 m AGL in Fairbanks.

Background air contains 30–40 nmol mol^{-1} O_3 in remote Alaska during winter (Oltmans & Komhyr, 1986). Emissions of nitric oxide (NO) will chemically remove (titrate) O_3 under polluted conditions through the reaction $NO + O_3 \rightarrow NO_2 + O_2$. Therefore, the direct result of pollution (NO emissions) is to reduce O_3, often to near-zero levels at night (Geyer & Stutz, 2004; Stutz et al., 2004; S. Wang et al., 2006; Wong et al., 2011). In this

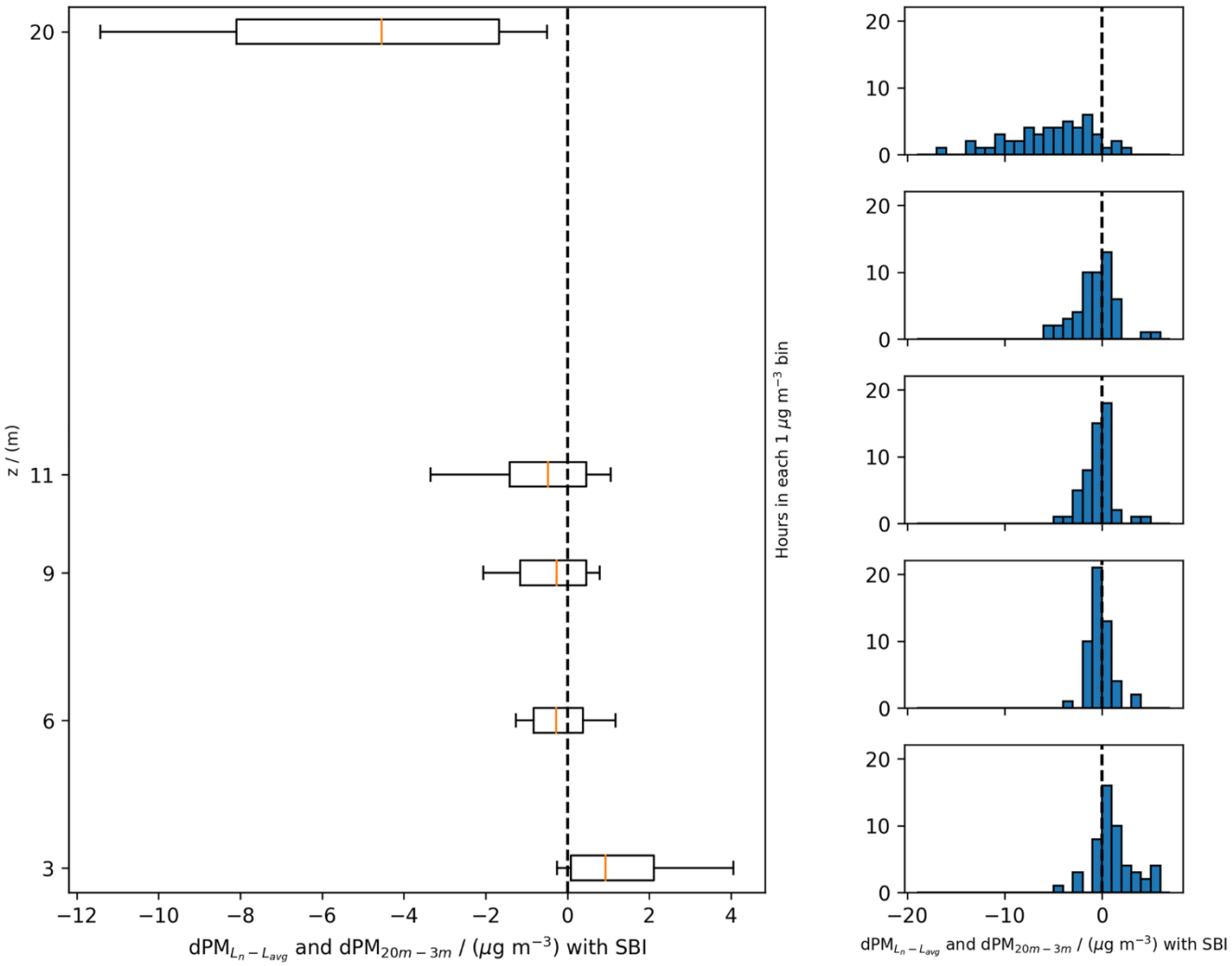

Figure 8. Box-and-whiskers plot of $dPM_{[Ln - Lavg]}$ when $dT_{11-3\ m} > 0.5$°C at the Trailer Tower and Community and Technical College building during the period of colocation; box edges show the 25th and 75th percentiles and whiskers show the 10th and 90th percentiles.

context, Figure 9 shows a similar vertical segregation effect for O_3, where O_3 is commonly removed at 3 m but less removed at 20 m. The frequency of large vertical O_3 mixing ratio differences also increased during SBIs. In Figure 10 and Table 4, selecting for SBIs increased the frequency of observation of observable vertical differences in O_3 ($dO3_{20-3\ m} > 2$ nmol mol^{-1}) from 26% to 48%. Due to the reduced vertical mixing during an SBI, pollution-emitted NO does not mix very far from the surface, so O_3 titration by NO will decrease as distance from the surface increases. In Fairbanks, full titration of O_3 is frequently observed at the surface, while air just 20 m aloft often has mixing ratios of 20–30 nmol mol^{-1} O_3.

In Utah's Salt Lake Valley, the pooling of cold air into large basins leads to strong SBIs in the winter with depths that often reach 500 m above the floor of the valley (Silcox et al., 2011). Silcox et al. (2011) found that $PM_{2.5}$ concentrations increased at a similar rate during SBIs at 10 sites spanning a roughly 500 m vertical scale across the Salt Lake Valley. These results are similar to those from Baasandorj et al. (2017) who measured similar $PM_{2.5}$ concentrations at three different sites spanning a roughly 200 m vertical scale in the Salt Lake Valley. Although $PM_{2.5}$ concentrations were similar across a 200-m vertical scale in the Salt Lake Valley, Baasandorj et al. (2017) measured vertical differences of O_3 and NO at night, where the site with the highest altitude in the valley had the smallest mixing ratios of NO and the largest mixing ratios of O_3.

During these nocturnal SBIs, NO_x (NO + NO_2) accumulates near the basin floor and O_3 is completely titrated by the large amounts of NO present. Figure 11 shows that the relationship between O_3 and $PM_{2.5}$ is similar at

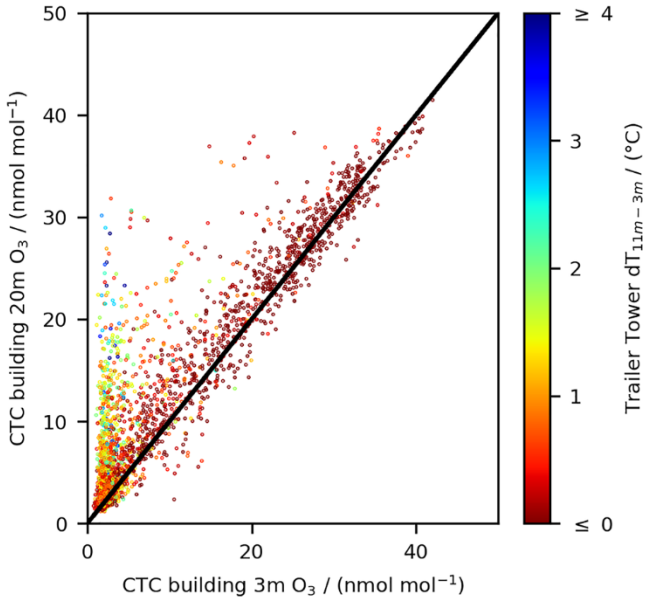

Figure 9. 20 versus 3 m O_3 at the Community and Technical College building colored by $dT_{11-3\,m}$ to show surface-based temperature inversion intensity.

both altitudes in Fairbanks as O_3 mixing ratios were zero in a majority of the data where $PM_{2.5}$ > 30 μg m^{-3} at both 3 and 20 m AGL. At 3 m AGL, measurements with strong SBIs generally had large $PM_{2.5}$ concentrations with O_3 mixing ratios near zero. In contrast, at 20 m AGL, there were many measurements that had moderate amounts of both $PM_{2.5}$ (10–20 μg m^{-3}) and O_3 (10–30 nmol mol^{-1}) present during strong SBIs. Although there were no measurements of NO_x at 20 m at the CTC building in Fairbanks, the more frequent presence of O_3 indicates that there was not enough NO injected into these air masses at 20 m to remove all O_3. In these moderately polluted but not fully titrated air masses, NO_2 and O_3 would coexist without NO, which are the appropriate conditions for the formation of nocturnal reactive nitrogen species, such as NO_3 and N_2O_5 (Atkinson et al., 1986).

In fully titrated air masses, excess NO is present, which reacts very rapidly with any NO_3 that may be formed (via reaction of NO and O_3) and short-circuits the formation of N_2O_5 (via a reversible reaction of NO_2 and NO_3) (Ayers & Simpson, 2006; S. G. Brown et al., 2006; S. S. Brown & Stutz, 2012; Geyer & Stutz, 2004; Joyce et al., 2014; Stutz et al., 2004). Hydrolysis of N_2O_5 can form HNO_3, which can increase amounts of nitrate in particulate matter, so this chemistry is of great interest for understanding secondary $PM_{2.5}$ formation. Therefore, the observed vertical differences in O_3 indicate that the chemical processing of pollution differs across the short vertical scale of 20 m AGL under cold, dark conditions. Suppression of nighttime N_2O_5 chemistry at the surface could be part of the reason for the low mass fraction of nitrate in Fairbanks particulate pollution (nitrate/$PM_{2.5}$ < 10% by mass) as compared to Salt Lake City, which experiences events with more than half of PM being ammonium nitrate (Alaska Department of Environmental Conservation, 2016; Nattinger, 2016; Utah Department of Environmental Quality, 2018). Model predictions indicate that if sufficient ammonia is present, the formation of ammonium nitrate may occur aloft above Fairbanks, facilitated by hindered vertical mixing (Joyce et al., 2014).

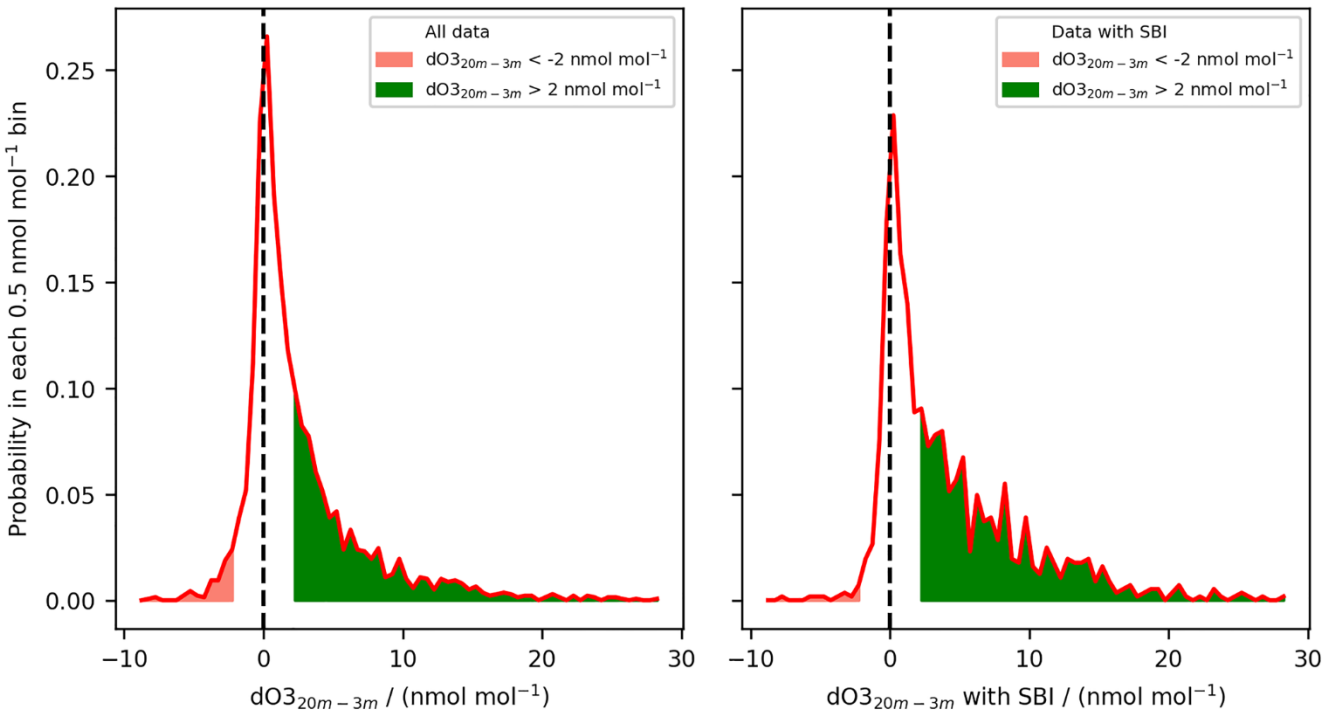

Figure 10. Histogram of O_3 differences $dO3_{20m-3m}$ at the Community and Technical College building. The left panel is all data, right panel is selected to have surface-based temperature inversion present.

Table 4
Percentage of Time O_3 Differences $dO3_{20-3\,m}$ Above or Below 2 ppb

	$dO3_{20-3\,m} > +2$ nmol mol^{-1}	$dO3_{20-3\,m} < -2$ nmol mol^{-1}
All data	26.3%	2.51%
Data with SBI	48.2%	0.97%

We expect at altitudes greater than 20 m aloft, there will be even larger mixing ratios of O_3 present since less primary NO emissions will be transported this far aloft during SBIs. With more O_3 expected at altitudes above 20 m, there is an even greater potential for secondary NO_x aerosol chemistry to occur. Nitrate that forms at higher altitudes has the potential to mix downward to the surface as the SBI dissipates; thus, nitrogen chemistry aloft could have an influence on particulate nitrate concentrations at the surface. In Beijing, the downward mixing of nitrate formed aloft at night was shown to have an impact on ground level $PM_{2.5}$ concentrations at sunrise, when nocturnal inversions were disrupted (H. Wang et al., 2018). A similar phenomenon could occur in Fairbanks when SBIs are disrupted.

Increased solar radiation in late winter (February and March) causes temperatures to rise during the day and drop at night in a diurnal cycle akin to what is seen in the lower latitudes. In Figure 2, there were a few times in late February and early March where this diurnal cycling occurred and caused SBIs to break during the day. Figure 12 compares two periods of diurnal cycling in Fairbanks during late winter, one from 2020 and one from 2019. The PurpleAir sensor at 3 m was not installed at the CTC building in 2019, so the average of three nearby PurpleAir monitors was taken for the 3 m data in 2019. Measurements of O_3 are not reported for 2019 as the O_3 analyzer was not yet installed at the CTC building.

In spring 2019, the diurnal temperature cycle appeared to have a greater impact on $PM_{2.5}$ concentrations as $PM_{2.5}$ differences were greatest at night and smallest during the day. Although there were certain times when $PM_{2.5}$ accumulated near the surface at night and cleared during the day, this diurnal pattern was not as dramatic in spring 2020 as it was in spring 2019. In Figure 13, the average diurnal cycle of $PM_{2.5}$ and temperature differences in spring 2019 appear similar to what is observed in the Salt Lake Valley during winter, where $PM_{2.5}$ differences are the largest at night when SBIs are present and decrease during the day as SBIs weaken. In this late winter scenario, daytime downwelling of nitrate that was formed aloft at night could add to the nitrate that is observed in $PM_{2.5}$ measured at the surface level. Additionally, secondary nitrate formed by this pathway may deposit regionally, acting as a nutrient to nitrogen-limited ecosystems (Fenn et al., 2003).

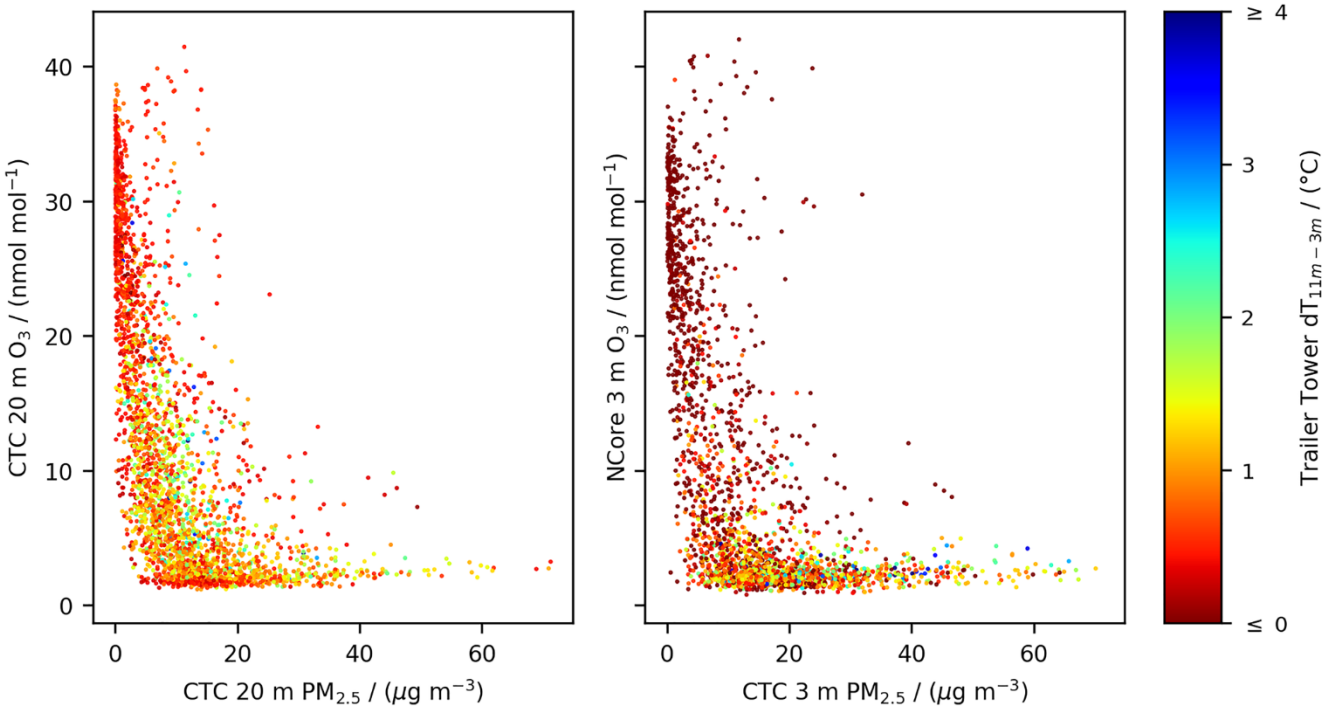

Figure 11. Correlation plot of O_3 versus $PM_{2.5}$ at 20 m above ground level (AGL, left) and 3 m AGL (right), colored by surface-based temperature inversion intensity.

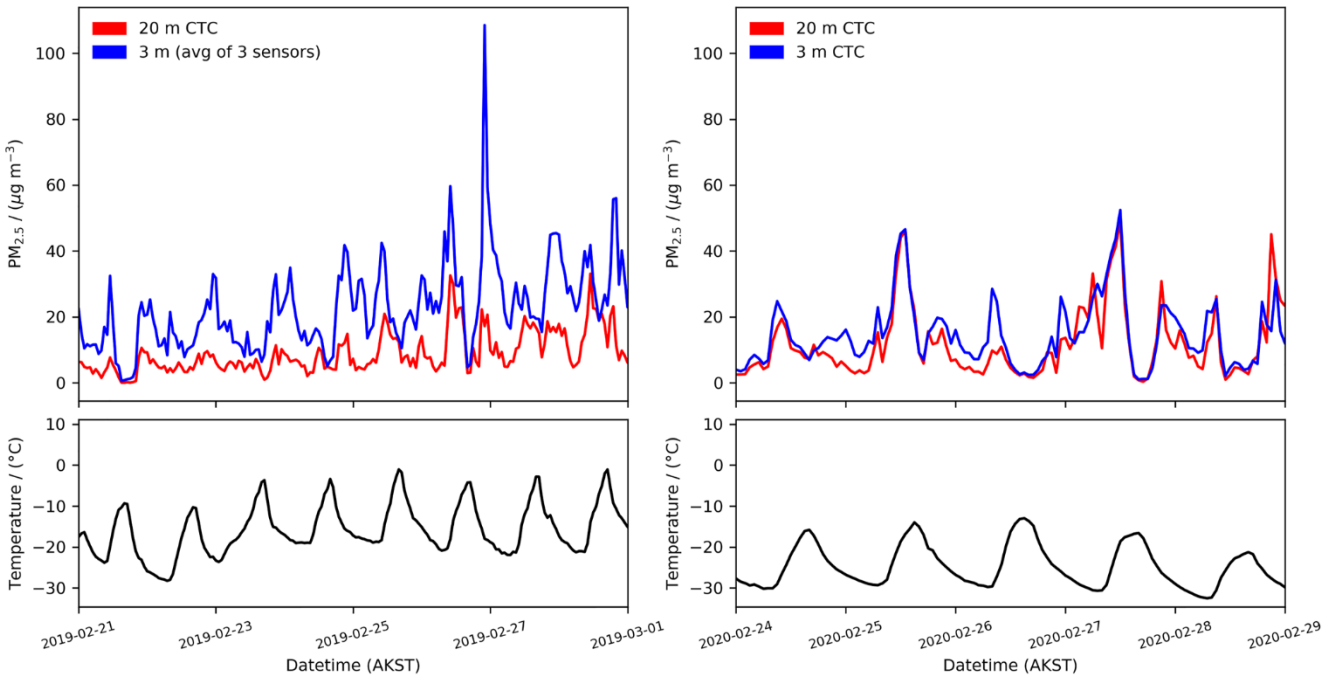

Figure 12. Comparison of two periods of time with a diurnal temperature cycle in 2019 (left) and 2020 (right).

Fairbanks shares conditions with many other high-latitude cities where it is cold in the winter and SBIs are common. Some basin areas in lower latitudes also share these cold, inverted conditions during winter nights, making this work clearly relevant to areas beyond Fairbanks. For example, in the Upper Silesia region of Poland, nocturnal SBIs were found to contribute to PM_{10} and $PM_{2.5}$ pollution events (Niedźwiedź et al., 2021). Situated in a circular mountain basin within the North China Plain, observations from Beijing in winter show that rapid

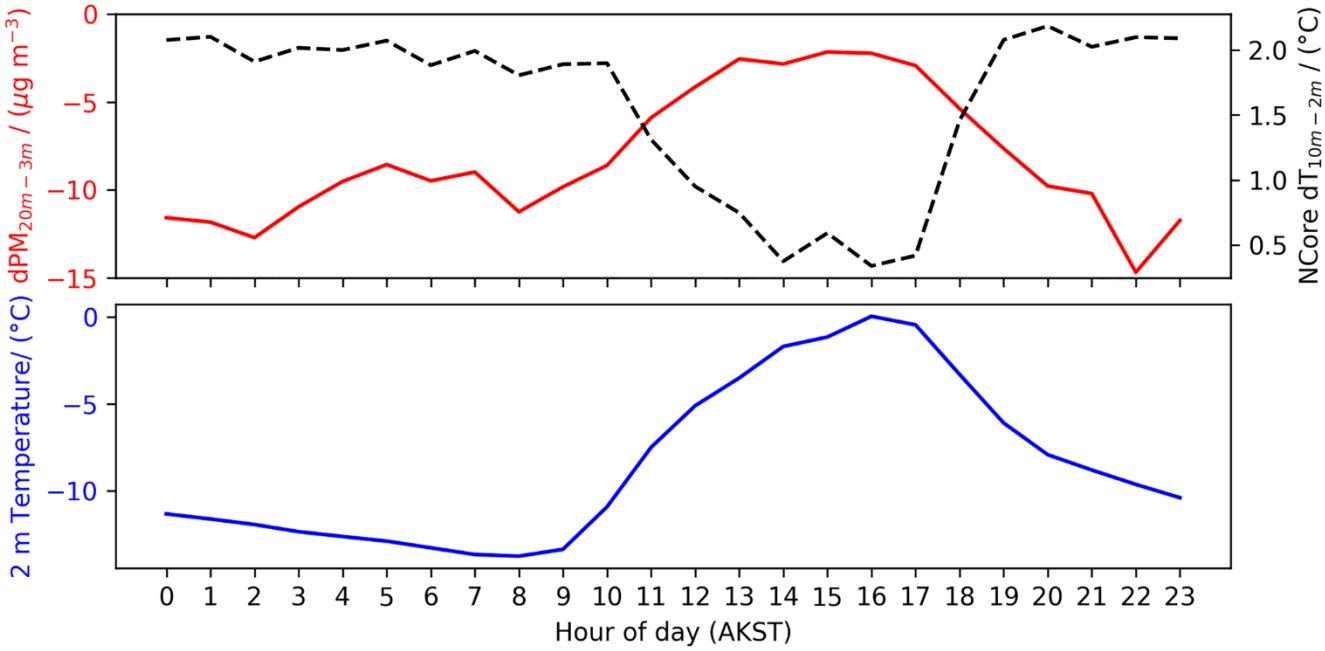

Figure 13. Average diurnal cycle of $PM_{2.5}$ differences at the Community and Technical College building ($dPM_{20-3\,m}$) and temperature difference from an Alaska Climate Research Center tower in Fairbanks ($dT_{10-2\,m}$) (top) and 2 m temperature from the Alaska Climate Research Center tower (located near the University of Alaska, Fairbanks, northwest of downtown). Data included from 21 February 2019 to 1 March 2019.

accumulation of $PM_{2.5}$ to unhealthy concentrations is associated with temperature inversion events during winter and an analysis of 5 years of radiosonde data from Northern China showed that 93% of severely polluted days were associated with temperature inversions (Xu et al., 2019; Zhong et al., 2017). Persistent wintertime temperature inversions are also related to the accumulation of PM10 pollution episodes in the Alpine Valleys near Grenoble, France (Largeron & Staquet, 2016).

While mixing layers may be taller in other areas (i.e., ~500 m), we clearly observe the lack of mixing for both $PM_{2.5}$ and O_3 across a 20-m vertical scale, so there are times when the mixed layer is shallower than 20 m in these data. Effectively, Fairbanks has very strong SBIs that limit the height of the mixed layer, which is a key result of our study. Although the 20-m vertical scale at which we see $PM_{2.5}$ and O_3 differences in Fairbanks may be very short, the change in O_3 mixing ratios and thus secondary aerosol NO_x chemistry during SBIs are a scenario that could also occur in many other parts of the world, likely on a taller vertical length scale than what is observed in Fairbanks.

5. Conclusion

In Fairbanks, Alaska, vertical differences in both $PM_{2.5}$ and O_3 were larger when SBIs were present, agreeing well with Tran and Mölders (2011), who found that $PM_{2.5}$ pollution events always occurred when SBIs with bases starting under 100 m were present. During SBIs, $PM_{2.5}$ concentrations were larger at 3 m than at 20 m and O_3 mixing ratios were near zero at 3 m, but often nonzero at 20 m. At 3 m, O_3 mixing ratios are small when $PM_{2.5}$ concentrations are large, while at 20 m, O_3 concentrations are larger, particularly when $PM_{2.5}$ concentrations are only moderately polluted.

The $PM_{2.5}$ from 3 to 11 m appeared to be more well-mixed than $PM_{2.5}$ from 3 to 20 m, as the median differences between each sensor on the 11-m Trailer Tower and the average of all Trailer Tower sensors were within ± 2 μg m^{-3}, while the median 20 m minus 3 m $PM_{2.5}$ difference at the CTC building was -4.8 μg m^{-3}. When there is little difference in $PM_{2.5}$ from 3 to 11 m, mechanical mixing near the surface may be influencing $PM_{2.5}$ concentrations, while episodic nonlinear $PM_{2.5}$ gradients at these altitudes may be influenced by home heating stack height effects.

The large differences in O_3 show that a distinct change in the oxidation regime in Fairbanks occurs between 20 and 3 m during SBIs. The presence of O_3 aloft has implications for nitrogen chemistry and particulate nitrate formation as NO_3 and N_2O_5 may be formed if both NO_x and O_3 are present at the same altitude. This work clearly indicates that the vertical length scale of pollution trapping during SBI conditions is very short with significant trapping in the lowest 20 m above the surface.

Acknowledgments
The winter 2019/2020 field study was funded with support by the US Army Garrison Alaska Fort Wainwright as well as the National Science Foundation (NSF) Sustainably Navigating Arctic Pollution Through Engaging Communities (SNAP-TEC) grant (NSF award number 1927750). An award from the University of Alaska Fairbanks Undergraduate Research and Scholarly Activity (URSA) was given in the spring of 2019 to support undergraduate research involved with this study. Tjarda J. Roberts and Kathy S. Law acknowledge funding support from the French National CNRS program LEFE (Les Enveloppes Fluides et l'Environnement), Institut Polaire Français—Paul-Emile Victor (IPEV), Observatoire de Versailles Saint-Quentin-en Yvelines (OVSQ), Orléans Labex Voltaire (ANR-10-LABX-100-0), and ANR PRC VOLC-HAL CLIM (ANR-18-CE01-0018).

Data Availability Statement

The $PM_{2.5}$, O_3 and temperature data in this study are available in text format in the ScholarWorks@UA institutional repository, URI: http://hdl.handle.net/11122/11344 (Simpson & Cesler-Maloney, 2020) or via email to the corresponding author.

References

Alaska Department of Environmental Conservation. (2016). *Amendments to: State air quality control plan*. Section III.D.5.1-5.14. Retrieved from https://dec.alaska.gov/media/6980/iii-d-05-pm25-sip-sections-adopted-090716.pdf

Ardon-Dryer, K., Dryer, Y., Williams, J. N., & Moghimi, N. (2020). Measurements of $PM_{2.5}$ with PurpleAir under atmospheric conditions. *Atmospheric Measurement Techniques*, *13*(10), 5441–5458. https://doi.org/10.5194/amt-13-5441-2020

Atkinson, R., Winer, A. M., & Pitts, J. M., Jr. (1986). Estimation of night-time N_2O_5 concentrations from ambient NO_2 and NO_3 radical concentrations and the role of N_2O_5 in night-time chemistry. *Atmospheric Environment*, *20*(2), 331–339. https://doi.org/10.1016/0004-6981(86)90035-1

Atkinson, R. W., Kang, S., Anderson, H. R., Mills, I. C., & Walton, H. A. (2014). Epidemiological time series studies of $PM_{2.5}$ and daily mortality and hospital admissions: A systematic review and meta-analysis. *Thorax*, *69*(7), 660–665. https://doi.org/10.1136/thoraxjnl-2013-204492

Ayers, J. D., & Simpson, W. R. (2006). Measurements of N_2O_5 near Fairbanks, Alaska. *Journal of Geophysical Research*, *111*(D14), D14309. https://doi.org/10.1029/2006jd007070

Baasandorj, M., Hoch, S. W., Bares, R., Lin, J. C., Brown, S. S., Millet, D. B., et al. (2017). Coupling between chemical and meteorological processes under persistent cold-air pool conditions: Evolution of wintertime $PM_{2.5}$ pollution events and N_2O_5 observations in Utah's Salt Lake Valley. *Environmental Science & Technology*, *51*(11), 5941–5950. https://doi.org/10.1021/acs.est.6b06603

Bi, J., Stowell, J., Seto, E. Y. W., English, P. B., Al-Hamdan, M. Z., Kinney, P. L., et al. (2020). Contribution of low-cost sensor measurements to the prediction of $PM_{2.5}$ levels: A case study in imperial county, California, USA. *Environmental Research*, *180*, 108810. https://doi.org/10.1016/j.envres.2019.108810

Bourne, S. M. (2008). *A climate perspective of observed and modeled surface-based temperature inversions in Alaska* (Master's thesis). University of Alaska Fairbanks. Retrieved from http://www.uaf.edu/asp/Students/theses/Bourne_SM.pdf

Bourne, S. M., Bhatt, U. S., Zhang, J., & Thoman, R. (2010). Surface-based temperature inversions in Alaska from a climate perspective. *Atmospheric Research*, *95*(2–3), 353–366. https://doi.org/10.1016/j.atmosres.2009.09.013

Brown, S. G., Roberts, P. T., McCarthy, M. C., Lurmann, F. W., & Hyslop, N. P. (2006). Wintertime vertical variations in particulate matter (PM) and precursor concentrations in the San Joaquin Valley during the California Regional Coarse PM/Fine PM Air Quality Study. *Journal of the Air & Waste Management Association*, *56*(9), 1267–1277. https://doi.org/10.1080/10473289.2006.10464583

Brown, S. S., & Stutz, J. (2012). Nighttime radical observations and chemistry. *Chemical Society Reviews*, *41*(19), 6405–6447. https://doi.org/10.1039/c2cs35181a

Busby, B. D., Ward, T. J., Turner, J. R., & Palmer, C. P. (2016). Comparison and evaluation of methods to apportion ambient $PM_{2.5}$ to residential wood heating in Fairbanks, AK. *Aerosol and Air Quality Research*, *16*(3), 492–503. https://doi.org/10.4209/aaqr.2015.04.0235

Carbone, S., Aurela, M., Saarnio, K., Saarikoski, S., Timonen, H., Frey, A., et al. (2014). Wintertime aerosol chemistry in sub-Arctic urban air. *Aerosol Science and Technology*, *48*(3), 313–323. https://doi.org/10.1080/02786826.2013.875115

Connell, D. P., Withum, J. A., Winter, S. E., Statnick, R. M., & Bilonick, R. A. (2005). The Steubenville Comprehensive Air Monitoring Program (SCAMP): Analysis of short-term and episodic variations in $PM_{2.5}$ concentrations using hourly air monitoring data. *Journal of the Air & Waste Management Association*, *55*(5), 559–573. https://doi.org/10.1080/10473289.2005.10464646

Dabek-Zlotorzynska, E., Dann, T. F., Kalyani Martinelango, P., Celo, V., Brook, J. R., Mathieu, D., et al. (2011). Canadian National Air Pollution Surveillance (NAPS) $PM_{2.5}$ speciation program: Methodology and $PM_{2.5}$ chemical composition for the years 2003–2008. *Atmospheric Environment*, *45*(3), 673–686. https://doi.org/10.1016/j.atmosenv.2010.10.024

Dominici, F., Peng, R. D., Bell, M. L., Pham, L., McDermott, A., Zeger, S. L., & Samet, J. M. (2006). Fine particulate air pollution and hospital admission for cardiovascular and respiratory diseases. *JAMA*, *295*(10), 1127–1134. https://doi.org/10.1001/jama.295.10.1127

Fenn, M. E., Baron, J. S., Allen, E. B., Rueth, H. M., Nydick, K. R., Geiser, L., et al. (2003). Ecological effects of nitrogen deposition in the western United States. *BioScience*, *53*(4), 404–420. https://doi.org/10.1641/0006-3568(2003)053[0404:eeondi]2.0.co;2

Fochesatto, G. J., & Mayfield, J. A. (2013). The layered structure of the winter atmospheric boundary layer in the interior of Alaska. *Journal of Applied Meteorology and Climatology*, *52*(4), 953–973. https://doi.org/10.1175/jamc-d-12-01.1

Geyer, A., & Stutz, J. (2004). Vertical profiles of NO_3, N_2O_5, O_3, and NO_x in the nocturnal boundary layer: 2. Model studies on the altitude dependence of composition and chemistry. *Journal of Geophysical Research*, *109*(D12), D12307. https://doi.org/10.1029/2003jd004211

Huang, W., Wang, G., Lu, S. E., Kipen, H., Wang, Y., Hu, M., et al. (2012). Inflammatory and oxidative stress responses of healthy young adults to changes in air quality during the Beijing Olympics. *American Journal of Respiratory and Critical Care Medicine*, *186*(11), 1150–1159. https://doi.org/10.1164/rccm.201205-0850OC

Joyce, P. L., von Glasow, R., & Simpson, W. R. (2014). The fate of NO_x emissions due to nocturnal oxidation at high latitudes: 1-D simulations and sensitivity experiments. *Atmospheric Chemistry and Physics*, *14*(14), 7601–7616. https://doi.org/10.5194/acp-14-7601-2014

Kankanala, P. (2007). *Doppler SODAR observations of the winds and structure in the lower atmosphere over Fairbanks, Alaska* (Master's thesis). University of Alaska Fairbanks. Retrieved from http://www.uaf.edu/asp/Students/theses/Pavan_thesis.pdf

Kossover, R. (2010). *Association between air quality and Hospital visits — Fairbanks, 2003–2008, Anchorage, AK*. Retrieved from http://www.epi.hss.state.ak.us/bulletins/docs/b2010_26.pdf

Kotchenruther, R. A. (2020). Recent changes in winter $PM_{2.5}$ contributions from wood smoke, motor vehicles, and other sources in the Northwest U.S. *Atmospheric Environment*, *237*, 117724. https://doi.org/10.1016/j.atmosenv.2020.117724

Largeron, Y., & Staquet, C. (2016). Persistent inversion dynamics and wintertime PM_{10} air pollution in Alpine valleys. *Atmospheric Environment*, *135*, 92–108. https://doi.org/10.1016/j.atmosenv.2016.03.045

Le Breton, M., Bacak, A., Muller, J. B. A., Bannan, T. J., Kennedy, O., Ouyang, B., et al. (2014). The first airborne comparison of N_2O_5 measurements over the UK using a CIMS and BBCEAS during the RONOCO campaign. *Analytical Methods*, *6*(24), 9731–9743. https://doi.org/10.1039/c4ay02273d

Nattinger, K. C. (2016). *Temporal and spatial trends of fine particulate matter composition in Fairbanks, Alaska* (Master's thesis). University of Alaska Fairbanks. Retrieved from https://scholarworks.alaska.edu/handle/11122/6830

Niedźwiedź, T., Łupikasza, E. B., Małarzewski, Ł., & Budzik, T. (2021). Surface-based nocturnal air temperature inversions in southern Poland and their influence on PM_{10} and $PM_{2.5}$ concentrations in Upper Silesia. *Theoretical and Applied Climatology*, *146*(3–4), 897–919. https://doi.org/10.1007/s00704-021-03752-4

Oltmans, S. J., & Komhyr, W. D. (1986). Surface ozone distributions and variations from 1973–1984: Measurements at the NOAA geophysical monitoring for climatic change baseline Observatories. *Journal of Geophysical Research*, *91*(D4), 5229–5236. https://doi.org/10.1029/JD091iD04p05229

Ouimette, J. R., Malm, W. C., Schichtel, B. A., Sheridan, P. J., Andrews, E., Ogren, J. A., & Arnott, W. P. (2021). Evaluating the PurpleAir monitor as an aerosol light. *Atmospheric Measurement Techniques*, *15*, 1–22. https://doi.org/10.5194/amt-15-1-2022

Pastuszka, J. S., Rogula-Kozlowska, W., & Zajusz-Zubek, E. (2010). Characterization of PM_{10} and $PM_{2.5}$ and associated heavy metals at the crossroads and urban background site in Zabrze, Upper Silesia, Poland, during the smog episodes. *Environmental Monitoring and Assessment*, *168*(1–4), 613–627. https://doi.org/10.1007/s10661-009-1138-8

Robinson, E., & Bell, G. J. (1956). Low-level temperature structure under Alaskan ice fog conditions. *American Meteorological Society Bulletin*, *37*(10), 506–513. https://doi.org/10.1175/1520-0477-37.10.506

Schmale, J., Arnold, S. R., Law, K. S., Thorp, T., Anenberg, S., Simpson, W. R., et al. (2018). Local Arctic air pollution: A neglected but serious problem. *Earth's Future*, *6*(10), 1385–1412. https://doi.org/10.1029/2018ef000952

Schmitt, C. G., Stuefer, M., Heymsfield, A. J., & Kim, C. K. (2013). The microphysical properties of ice fog measured in urban environments of Interior Alaska. *Journal of Geophysical Research: Atmospheres*, *118*(19), 11136–11147. https://doi.org/10.1002/jgrd.50822

Silcox, G. D., Kelly, K. E., Crosman, E. T., Whiteman, C. D., & Allen, B. L. (2011). Wintertime $PM_{2.5}$ concentrations during persistent, multi-day cold-air pools in a mountain valley. *Atmospheric Environment*, *46*, 17–24. https://doi.org/10.1016/j.atmosenv.2011.10.041

Silkoff, P. E., Zhang, L., Dutton, S., Langmack, E. L., Vedal, S., Murphy, J., & Make, B. (2005). Winter air pollution and disease parameters in advanced chronic obstructive pulmonary disease panels residing in Denver, Colorado. *The Journal of Allergy and Clinical Immunology*, *115*(2), 337–344. https://doi.org/10.1016/j.jaci.2004.11.035

Simpson, W., & Cesler-Maloney, M. (2020). Gas and particle data from Fairbanks during the winter of 2019/2020 [Dataset]. . Retrieved from http://hdl.handle.net/11122/11344

Smoot, A. R., & Thomas, C. K. (2013). An effective, economic, aspirated radiation shield for air temperature observations and its spatial gradients. *Journal of Atmospheric and Oceanic Technology*, *30*(3), 526–537. https://doi.org/10.1175/jtech-d-12-00044.1

Stutz, J., Alicke, B., Ackermann, R., Geyer, A., White, A., & Williams, E. (2004). Vertical profiles of NO_3, N_2O_5, O_3, and NO_x in the nocturnal boundary layer: 1. Observations during the Texas air quality study 2000. *Journal of Geophysical Research*, *109*(D12), D12306. https://doi.org/10.1029/2003jd004209

Tran, H. N. Q., & Mölders, N. (2011). Investigations on meteorological conditions for elevated $PM_{2.5}$ in Fairbanks, Alaska. *Atmospheric Research*, *99*(1), 39–49. https://doi.org/10.1016/j.atmosres.2010.08.028

Tran, H. N. Q., & Mölders, N. (2012). Numerical investigations on the contribution of point source emissions to the $PM_{2.5}$ concentrations in Fairbanks, Alaska. *Atmospheric Pollution Research*, *3*(2), 199–210. https://doi.org/10.5094/apr.2012.022

Tsybulski Gennady, G. M., Dergunov, A., Yakubailik, O., Noskov, M. V., & Maglinets, Y. A. (2020). Analysis of temperature inversions during periods of adverse weather conditions in Krasnoyarsk in the winter period of 2019–2020. In *E3S Web of Conferences* (Vol., 223, p. 03021). EDP Sciences. https://doi.org/10.1051/e3sconf/202022303021

Utah Department of Environmental Quality, D. (2018). *Utah state implementation plan: Control measures for area and point sources, fine particulate matter, serious area $PM_{2.5}$ SIP for the Salt Lake city, UT nonattainment area, Section IX. Part A. 31, 6*. Retrieved from https://documents.deq.utah.gov/air-quality/pm25-serious-sip/DAQ-2018-013088.pdf

Wang, H., Lu, K., Chen, X., Zhu, Q., Wu, Z., Wu, Y., & Sun, K. (2018). Fast particulate nitrate formation via N_2O_5 uptake aloft in winter in Beijing. *Atmospheric Chemistry and Physics*, *18*(14), 10483–10495. https://doi.org/10.5194/acp-18-10483-2018

Wang, S., Ackermann, R., & Stutz, J. (2006). Vertical profiles of O_3 and NO_x chemistry in the polluted nocturnal boundary layer in Phoenix, AZ: I. Field observations by long-path DOAS. *Atmospheric Chemistry and Physics*, *6*(9), 2671–2693. https://doi.org/10.5194/acp-6-2671-2006

Wang, Y., & Hopke, P. K. (2014). Is Alaska truly the great escape from air pollution? – Long term source apportionment of fine particulate matter in Fairbanks, Alaska. *Aerosol and Air Quality Research*, *14*(7), 1875–1882. https://doi.org/10.4209/aaqr.2014.03.0047

Ward, T., Trost, B., Conner, J., Flanagan, J., & Jayanty, R. K. M. (2012). Source apportionment of $PM_{2.5}$ in a subarctic airshed - Fairbanks, Alaska. *Aerosol and Air Quality Research*, *12*(4), 536–543. https://doi.org/10.4209/aaqr.2011.11.0208

Wendler, G., & Jayaweera, K. O. L. F. (1972). Some measurements on the development of the surface inversion in Central Alaska during winter. *Pure and Applied Geophysics*, *99*(1), 209–221. https://doi.org/10.1007/bf00875277

Wong, K. W., Oh, H. J., Lefer, B. L., Rappenglück, B., & Stutz, J. (2011). Vertical profiles of nitrous acid in the nocturnal urban atmosphere of Houston, TX. *Atmospheric Chemistry and Physics*, *11*(8), 3595–3609. https://doi.org/10.5194/acp-11-3595-2011

Xu, T., Song, Y., Liu, M., Cai, X., Zhang, H., Guo, J., & Zhu, T. (2019). Temperature inversions in severe polluted days derived from radiosonde data in North China from 2011 to 2016. *Science of the Total Environment*, *647*, 1011–1020. https://doi.org/10.1016/j.scitotenv.2018.08.088

Zhong, J., Zhang, X., Wang, Y., Sun, J., Zhang, Y., Wang, J., et al. (2017). Relative contributions of boundary-layer meteorological factors to the explosive growth of $PM_{2.5}$ during the red alert heavy pollution episodes in Beijing in December 2016. *Journal of Meteorological Research*, *31*(5), 809–819. https://doi.org/10.1007/s13351-017-7088-0

References From the Supporting Information

Andreas, E. L., Guest, P. S., Persson, P. O. G., Fairall, C. W., Horst, T. W., Moritz, R. E., & Semmer, S. R. (2002). Near-surface water vapor over polar sea ice is always near ice saturation. *Journal of Geophysical Research*, *107*(C10), 8033. https://doi.org/10.1029/2000jc000411

Kelly, K. E., Whitaker, J., Petty, A., Widmer, C., Dybwad, A., Sleeth, D., et al. (2017). Ambient and laboratory evaluation of a low-cost particulate matter sensor. *Environmental Pollution*, *221*, 491–500. https://doi.org/10.1016/j.envpol.2016.12.039

Wallace, L., Bi, J., Ott, W. R., Sarnat, J., & Liu, Y. (2021). Calibration of low-cost PurpleAir outdoor monitors using an improved method of calculating PM. *Atmospheric Environment*, *256*, 118432. https://doi.org/10.1016/j.atmosenv.2021.118432